

# Journal of Materials Chemistry A

Accepted Manuscript



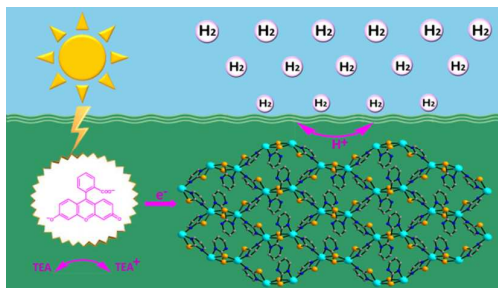
This is an *Accepted Manuscript*, which has been through the Royal Society of Chemistry peer review process and has been accepted for publication.

*Accepted Manuscripts* are published online shortly after acceptance, before technical editing, formatting and proof reading. Using this free service, authors can make their results available to the community, in citable form, before we publish the edited article. We will replace this *Accepted Manuscript* with the edited and formatted *Advance Article* as soon as it is available.

You can find more information about *Accepted Manuscripts* in the [Information for Authors](#).

Please note that technical editing may introduce minor changes to the text and/or graphics, which may alter content. The journal's standard [Terms & Conditions](#) and the [Ethical guidelines](#) still apply. In no event shall the Royal Society of Chemistry be held responsible for any errors or omissions in this *Accepted Manuscript* or any consequences arising from the use of any information it contains.

## Graphical Abstract



A 2D Ni/S MOF was prepared to function as an efficient heterogeneous catalyst for sunlight-driven hydrogen production in water.

# Application of a Ni mercaptopyrimidine MOF as highly efficient catalyst for sunlight-driven hydrogen generation

Cite this: DOI: 10.1039/x0xx00000x

Yanan Feng,<sup>ac</sup> Chi Chen,<sup>b</sup> Zhuguang Liu,<sup>d</sup> Binjie Fei,<sup>d</sup> Ping Lin,<sup>a</sup> Qipeng Li,<sup>a</sup> Shigang Sun<sup>b</sup> and Shaowu Du<sup>\*a</sup>

Received 00th January 2012,  
Accepted 00th January 2012

DOI: 10.1039/x0xx00000x

www.rsc.org/

Microscale crystals of a 2D layered MOF  $[\text{Ni}_2(\text{PymS})_4]_n$  (PymSH = Pyrimidine-2-thio) with a thiolate-bridged binuclear Ni(II) node similar to the active site of the [NiFe]-hydrogenase were prepared. This material shows high catalytic activity for the visible-light-driven hydrogen production under the illumination of white LED or direct sunlight. The turnover frequency (TOF) of the catalyst can reach up to  $10.6 \text{ h}^{-1}$ . The heterogeneous nature and recyclability of the catalyst, as well as factors that affect the catalytic activity were investigated and described. Moreover, the photocatalytic mechanism for the hydrogen generation of  $[\text{Ni}_2(\text{PymS})_4]_n$  was also proposed based on the fluorescence spectra and cyclic voltammetry.

## Introduction

Hydrogen is a promising alternative to replace fossil fuels with no carbon and high specific enthalpy of combustion. Exploring the way to produce hydrogen at large scale has long been a topic of extensive research worldwide. Massive studies are focused on the photolysis of water to produce hydrogen aiming to utilize the abundant solar energy resources on earth.<sup>1-3</sup> In the system of photocatalysis for hydrogen production, three components are typically involved. The first is photosensitizers (PSs) which are used to capture solar photons and release photoelectrons. Semiconductor nanocrystals,<sup>4, 5</sup> organic dyes<sup>6</sup> and organometallic compounds<sup>7, 8</sup> are common to function as PSs with excellent performance. The second is sacrificial electron donors which provide electrons for PSs. The last is catalysts that serve as electron acceptors and catalyse protons to release hydrogen. Noble metals such as platinum are considered as superior catalysts in this system and have long been used in practice. Unfortunately, the low abundance and high cost of noble metals greatly restrain their further development. In recent years, several catalytic systems using only earth-abundant transition metals such as Fe, Co and Ni have been developed for photo-generation of hydrogen. Some of them, in particular those that mimic the active sites of natural hydrogenases have been found to perform efficient and robust ability in catalytic hydrogen production.<sup>5, 9-12</sup> However, most of these systems are operated in mixed organic-aqueous solutions and the difficulty in reuse is their common defect. Furthermore, little has been reported on the utilization of direct sunlight. Therefore, exploring a new system for actual sunlight-driven

hydrogen evolution utilizing water-stable and recoverable catalysts may have great practical significance.

Metal-organic frameworks (MOFs) are a class of crystalline materials constructed by nodes of metal ions or clusters and organic linkers. Their structural diversity, huge specific surface area and pore volumes make them interesting for several applications such as chemical sensing, gas storage/separation, luminescence, magnetism, and so on.<sup>13-15</sup> At present, their possible applications have been extended to the field of heterogeneous catalysis by either introducing catalytically active sites into the framework or by using secondary building units (e.g. metal-oxo clusters) as active sites.<sup>16-21</sup> In the former case, the MOFs only function as supporters or containers to encapsulate small micromolecular catalysts or metal nanoparticles. In the latter case, the active species can be designed as nodes and integrated into one- or two-dimensional MOFs to improve the catalytic activity and enhance their insolubility and stability, as well as their capability of reuse.

With this in mind, we synthesized herein a 2D water-stable MOF, formulated as  $[\text{Ni}_2(\text{PymS})_4]_n$  (PymSH = Pyrimidine-2-thiol),<sup>22</sup> in which the binuclear  $[\text{Ni}_2\text{S}]$  node is structurally similar to that of the active site of the [NiFe]-hydrogenase (Fig. 1a)<sup>23</sup>. The two-dimensional architecture of  $[\text{Ni}_2(\text{PymS})_4]_n$  (Fig. 1b) can not only increase the exposure of active nodes to the substrates, but also lead to high stability and insolubility in water, which enable it to be a potential heterogeneous catalyst for hydrogen production under aqueous condition. In this paper, we reported the synthesis of  $[\text{Ni}_2(\text{PymS})_4]_n$  with various particle sizes by careful regulating the synthetic conditions. The effects of catalyst particle size and other factors to the productivity of

hydrogen, the photo-induced electron transfer pathway and the process of electrocatalytic proton reduction in water were also studied.

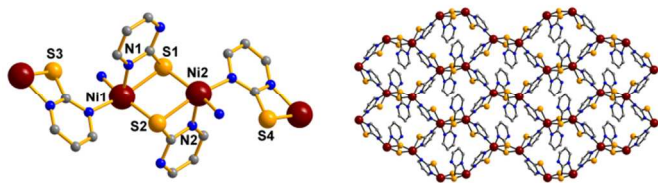


**Fig. 1** The basic structural unit (left) and 2D lamellar structure (right) of  $[\text{Ni}_2(\text{PymS})_4]_n$ .

## Experimental section

### Materials and characterization

All the chemicals were purchased and used without further purification. The white LED light was purchased from Cree Company and driven by Antai regulated power supply. Powder X-ray diffraction (PXRD) patterns were recorded on a Rigaku MiniFlex diffractometer with crushed single crystals in the  $2\theta$  range from 5 to  $60^\circ$ . Thermo-gravimetric experiments were performed using a TGA/Netsch STA 449C instrument heated from 30 to  $1000^\circ\text{C}$  (heating rate of  $10^\circ\text{C min}^{-1}$ , nitrogen or oxygen stream). Fluorescence quenching experiments were carried out on a Cary Eclipse fluorescence spectrometer. The pH values were measured by a Sartorius PB-10 pH meter. The leaching test was carried on the Ultima inductively coupled plasma OES spectrometer (ICP-OES).

### Photocatalysis

In a typical photocatalytic experiment, an aqueous triethylamine (TEA) solution with an adjusted pH value was added to the mixture of a ground sample of  $[\text{Ni}_2(\text{PymS})_4]_n$  and fluorescein (FI) in a Schlenk tube to keep the volume at 5 mL. The solution was degassed by three freeze-pump-thaw cycles before illuminated from below with a Cree XML2 white-light-diode (LED). The light power was set to 2.02 W and measured with a Yuanfang PMS-80\_V1 system. The hydrogen was monitored by gas chromatograph (Fuli 9790II) equipped with a thermal conductivity detector and a  $5 \text{ \AA}$  molecular column ( $\Phi 3 \text{ mm} \times 3 \text{ m}$ ) heated at 353 K under argon.

### Electrochemistry

Electrochemical experiments were carried out on a CHI 760D electrochemical potentiostat. Cyclic voltammograms were recorded in a three-electrode cell under  $\text{N}_2$  with a glassy carbon disc (diameter 5 mm) as working electrode, a saturated calomel electrode as reference electrode and a platinum sheet as auxiliary electrode. A 0.1M sodium perchlorate solution was used as electrolyte. The sample  $[\text{Ni}_2(\text{PymS})_4]_n$  (10 mg) was dispersed in a mixture of water (1 mL) and Nafion (5%, 50  $\mu\text{L}$ ) before ultrasonicated for 30 min. Afterwards, 10  $\mu\text{L}$  of the resultant mixture was applied to the surface of glassy carbon.

After drying under illumination of infrared lamp, Nafion (0.05%, 10  $\mu\text{L}$ ) in ethanol was coated on the surface of the catalyst and dried again before the electrochemical test.

### Fluorescence Quenching

The emission spectra of the aqueous fluorescence solution (0.01 mM) with different concentrations of  $[\text{Ni}_2(\text{PymS})_4]_n$  or TEA was excited at 460 nm with a flash xenon lamp and detected by R928 photomultiplier detector on a Cary Eclipse fluorescence spectrometer.

### Synthesis of $[\text{Ni}_2(\text{PymS})_4]_n$

$\text{Ni}(\text{Ac})_2 \cdot 4\text{H}_2\text{O}$  (107 mg, 0.45 mmol), KOH (56 mg, 0.9 mmol) and 2-mercapto-pyrimidine (100 mg, 0.9 mmol) was placed in a 23 mL Teflon-lined stainless steel reactor with 8 mL of water. The mixture was heated to 348 K within 2 hours and kept at this temperature for 6 hours, then cooled to 323 K in another 5 hours. Green crystals of  $[\text{Ni}_2(\text{PymS})_4]_n$  with the size around  $4 \times 1 \times 4 \mu\text{m}$  (length  $\times$  width  $\times$  height) were collected and washed with water followed by alcohol several times and dried in air (yield: 60 mg, 47%). FT-IR (KBr pallet): 1637 (w), 1571 (m), 1540 (s), 1432(w), 1375 (s), 1234 (w), 1204 (w), 1173 (m), 1075 (w), 988 (w), 971 (w), 809 (w), 792 (w), 765 (w), 752 (m), 668 (w), 658 (w)  $\text{cm}^{-1}$ . Extended the reaction time to 12 hours gave larger crystals (*ca.*  $11 \times 4 \times 10 \mu\text{m}$ ). Crystals with the size around  $20 \times 4 \times 10 \mu\text{m}$  can be obtained by raising the reaction temperature to 393 K and cooling the reaction mixture to 373 K in 24 hours and then to 303 K in another 24 hours.

## Results and discussion

A sample of  $[\text{Ni}_2(\text{PymS})_4]_n$  was prepared by the hydrothermal reaction of  $\text{Ni}(\text{Ac})_2 \cdot 4\text{H}_2\text{O}$ , KOH and 2-mercapto-pyrimidine in a molar ratio of 1:2:2 in water at 348 K for 6 hours. Field-emission scanning electron microscopy (FE-SEM) reveals the layered deposited, spindly crystals of  $[\text{Ni}_2(\text{PymS})_4]_n$  with the size around  $4 \times 1 \times 4 \mu\text{m}$  (length  $\times$  width  $\times$  height) (Fig. 2a). By careful adjusting the reaction temperature and time, we were able to obtain a series of green crystals with different sizes (Fig. 2b and 2c).

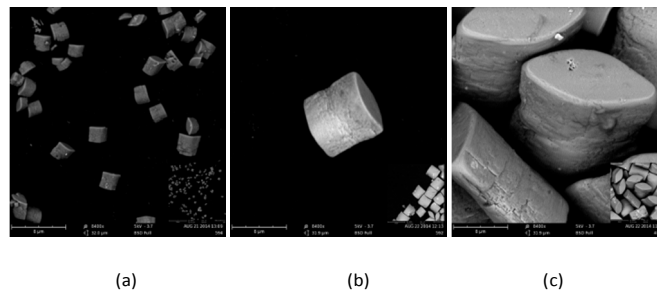


**Fig. 2** FE-SEM image of  $[\text{Ni}_2(\text{PymS})_4]_n$  with different sizes: (a)  $4 \times 1 \times 4 \mu\text{m}$ ; (b)  $11 \times 4 \times 10 \mu\text{m}$ ; (c)  $20 \times 4 \times 10 \mu\text{m}$ . The outlet scale is 8  $\mu\text{m}$  and the inlet scale is 20  $\mu\text{m}$ .

Compound  $[\text{Ni}_2(\text{PymS})_4]_n$  possesses a 2D lamellar structure built up from binuclear nodes  $[\text{Ni}_2(\text{PymS})_4]$ , in which the Ni(II)

ions are in turn connected by  $\text{PymS}^-$  ligands through  $S$  and  $N$  atoms to form inorganic and organic layers (Fig. 1). Each binuclear node is composed of two Ni(II) ions and four  $\text{PymS}^-$  ligands, in which two ligands bridge the Ni(II) ions while the other two each terminally coordinates to one of the Ni(II) ions through  $S$  atom, similar to the bridging and terminal cysteine residues coordinated to the metal ions in the active centre of [NiFe]-hydrogenases and other mimics.<sup>23, 24</sup> Such a 2D netted structure offers superior stability in comparison with biological or micromolecular mimics, especially in an oxygen atmosphere. As illustrated in Fig. 3a, compound  $[\text{Ni}_2(\text{PymS})_4]_n$  does not decompose in the presence of either air or nitrogen until the temperature rises up to 300°C and can be stored in air at ambient temperature for months. Moreover, after being soaked in water with a wide pH range for five days, little change was observed in the XRD spectra (Fig. 3b), which indicated the noticeable durability of  $[\text{Ni}_2(\text{PymS})_4]_n$  to both acid and basic solutions.

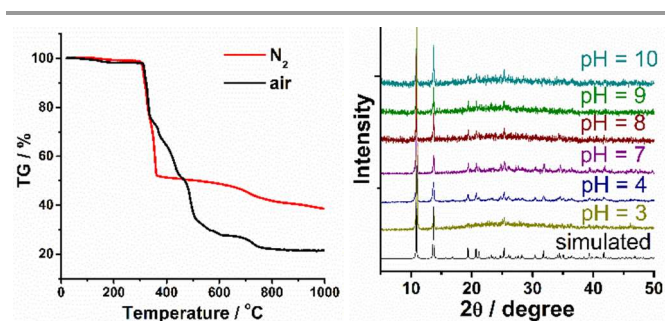


**Fig. 3** (left) Thermal gravimetric analysis of  $[\text{Ni}_2(\text{PymS})_4]_n$  in the presence of air (black line) and nitrogen (red line); (right) powder XRD patterns of  $[\text{Ni}_2(\text{PymS})_4]_n$  after soaked in water for five days with varied pH values adjusted by concentrated hydrochloric acid and TEA.

**Table 1** The amount of hydrogen evolved with varied photosensitizers and electron donors.

Cat	PS	Electron donor	$\text{H}_2$ ( $\mu\text{mol}$ )
$[\text{Ni}_2(\text{PymS})_4]_n$ [a]	Eosin Y	TEA <sup>[e]</sup>	0.28
$[\text{Ni}_2(\text{PymS})_4]_n$ [a]	Rhodamine B	TEA <sup>[e]</sup>	0.1
$[\text{Ni}_2(\text{PymS})_4]_n$ [a]	Erythrosin B	TEA <sup>[e]</sup>	1.8
$[\text{Ni}_2(\text{PymS})_4]_n$ [a]	$\text{Ru}(\text{bpy})_3\text{Cl}_2$	TEA <sup>[e]</sup>	0.45
$[\text{Ni}_2(\text{PymS})_4]_n$ [a]	Fl	TEA <sup>[e]</sup>	22.3
$[\text{Ni}_2(\text{PymS})_4]_n$ [a]	Fl	TEA <sup>[f]</sup>	33.7
$[\text{Ni}_2(\text{PymS})_4]_n$ [a]	Fl	TEOA <sup>[g]</sup>	0.15
$[\text{Ni}_2(\text{PymS})_4]_n$ [b]	Fl	TEA <sup>[f]</sup>	35.7
$\text{NiCl}_2 \cdot 6\text{H}_2\text{O}$ [c]	Fl	TEA <sup>[f]</sup>	0.62
$\text{PymSH}$ [d]	Fl	TEA <sup>[f]</sup>	0.23

The experiments were carried out at room temperature with different catalysts, PSs and electron donors for one hour. [a]  $[\text{Ni}_2(\text{PymS})_4]_n$  (2.8 mg). [b]  $[\text{Ni}_2(\text{PymS})_4]_n$  (5.6 mg). [c]  $\text{NiCl}_2 \cdot 6\text{H}_2\text{O}$  (2 mM). [d]  $\text{PymSH}$  (2 mM). [e] TEA (5%, v/v). [f] TEA (15%, v/v). [g] TEOA (15%, v/v).

Photocatalytic experiments were performed in water at room temperature with white-light-diode (LED) working as the light

source. In the photocatalytic system,  $[\text{Ni}_2(\text{PymS})_4]_n$  worked as the catalyst, fluorescein (Fl) as the photosensitizer and TEA as the electron donor. All of the three components were essential as the absence of any one of them would lead to no hydrogen generation. In addition, this system produces hydrogen only under illumination. When LED light was turned off, hydrogen evolution ceased. When tiny amount of  $[\text{Ni}_2(\text{PymS})_4]_n$  (1.4 mg) was used, significant amount of hydrogen was detected within an hour. The turnover frequency (TOF) was calculated to be  $10.6 \text{ h}^{-1}$ , which is higher than some photocatalytic systems using MOFs with either noble or non-noble metals.<sup>25</sup> To verify that  $[\text{Ni}_2(\text{PymS})_4]_n$  was indeed participated in the photocatalytic reaction, contrast experiments were conducted by replacing the catalyst with equal mole of nickel chloride and  $\text{PymSH}$ , respectively. The amount of hydrogen detected in both cases was much less than that using  $[\text{Ni}_2(\text{PymS})_4]_n$  as a catalyst (Table 1).

After the photocatalyzed reaction, the catalyst was recovered by centrifugation and subjected to FT-IR and powder XRD measurements, respectively. Little change was observed in both the FT-IR and XRD spectra (Fig. S2). The recovered catalyst was added to a fresh solution of TEA and Fl and illuminated again, hydrogen was regenerated with the similar rate as before (Fig. 4). Under the same treatment, the catalyst could be used repeatedly for four catalytic cycles. However, as can be seen in Table S1, a decreased performance in hydrogen generation was observed during the recyclability tests.

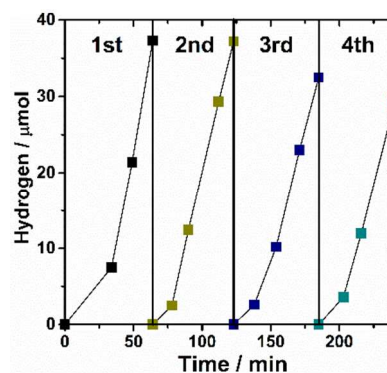


**Fig. 4** Volume of hydrogen photogenerated in the presence of complex  $[\text{Ni}_2(\text{PymS})_4]_n$  (15  $\mu\text{mol}$ ) with re-addition of Fl (2 mM) and TEA (15%, v/v) in water.

After adding  $[\text{Ni}_2(\text{PymS})_4]_n$  to a water solution containing TEA and Fl and stirring the mixture for five minutes, the supernatant was separated by centrifugation and illuminated by a LED for an hour. Only trace of hydrogen was produced (Fig. S1). Besides, the Ni leaching after one catalytic run was 2.3% confirmed by ICP-OES. These results indicate the non-homogeneous nature of the catalyst. Remarkably, this system can also produce hydrogen under the direct sunlight. A mixture of  $[\text{Ni}_2(\text{PymS})_4]_n$ , Fl and TEA in an aqueous solution at pH = 10 was placed under direct sunlight outdoors. After an hour, about 6  $\mu\text{mol}$  hydrogen was detected (Fig. 5), which realizes the actual solar-to-chemical conversion.



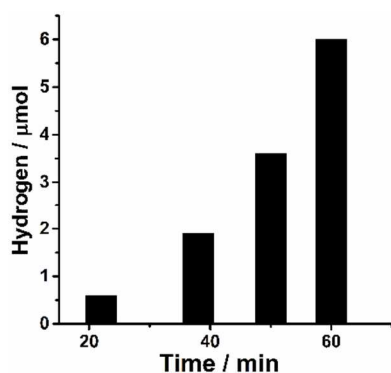


**Fig. 5** The amount of hydrogen photogenerated in the presence of  $[\text{Ni}_2(\text{PymS})_4]_n$  (10  $\mu\text{mol}$ ), FI (2 mM) and TEA (15%) in water under the illumination of sunlight in Fuzhou city from 11:30 to 12:30 on Nov 2, 2014.

In order to investigate the factors that affect the activity of  $[\text{Ni}_2(\text{PymS})_4]_n$ , we first compared its catalytic ability in water at different pH values. Several photocatalytic experiments were conducted in water with the pH values varied from 7 to 10. As seen in Fig. S3, both the initial rate and the amount of hydrogen reduced with the decreasing pH value. When the pH value was equal or less than 8, no hydrogen was measured. This could be because more TEA is protonated at low pH, which diminished its electron-donating ability in the photocatalytic circulation and led to no hydrogen production.<sup>12b</sup>

As a significant component in the photocatalytic system, the sacrificial electron donor is also an important factor that affects the activity of catalyst. TEA is one of the common electron donors in basic condition. It is slightly soluble in water above 18.7°C. At room temperature, homogeneous solution was obtained when TEA and water were mixed with varied ratios from 1/20 to 1/10. When the ratio increased to 3/20, the mixture layered. However, as the pH value was adjusted to 10 or lower by adding concentrated hydrochloric acid, the layered solution mixed uniformly. As shown in Fig. S4, more hydrogen was generated and a slightly faster initial rate was observed with increasing volume ratio of TEA and water from 1/20 to 3/20. In addition, under the same conditions, very little hydrogen (0.15  $\mu\text{mol}$ ) was detected when triethanolamine (TEOA), which is another common electron donor in the photocatalytic system with better solubility in water, was used instead of TEA (Table 1).

Furthermore, the effect of sensitizer also cannot be neglected on the photocatalytic reaction. In spite of good performance of Eosin B, erythrosine and rhodamine B in other photocatalytic systems, replacing FI with these sensitizers greatly reduced the amount of hydrogen evolved (Table 1). The same applies to the classic sensitizer,  $\text{Ru}(\text{bpy})_3\text{Cl}_2$ . When it was used to replace FI, just 0.45  $\mu\text{mol}$  of hydrogen was detected, much less than the value of 22.3  $\mu\text{mol}$  with FI. Meanwhile, the concentration of FI is another significant influential factor. When the concentration of FI was increased from 2 to 10 mM, the amount of hydrogen produced decreased from 33.7 to 10.2  $\mu\text{mol}$  (Fig. S5). This phenomenon could be due to the aggregation-caused quenching

(ACQ).<sup>26</sup> High concentration of FI may cause self-quenching of  $\text{FI}^*$  and reduce its opportunity of being quenched by electron transfer (ET). Thus, the yield decreased as the concentration of FI increased.

Finally, the amount of hydrogen photoevolved is also related to the quantity of catalyst used and the particle sizes of catalyst. When the concentration of FI and TEA was fixed, the amount of catalyst made a significant influence on the generation of hydrogen. With an increasing dosage of the catalyst from 1.4 to 11.2 mg, the hydrogen production raised subsequently, whereas the TOF decreased instead (Fig. 6, Table S2). When equal amounts of the catalyst were used under the same conditions, the smaller the particle size of catalyst was, the more hydrogen was produced (Fig. S6).

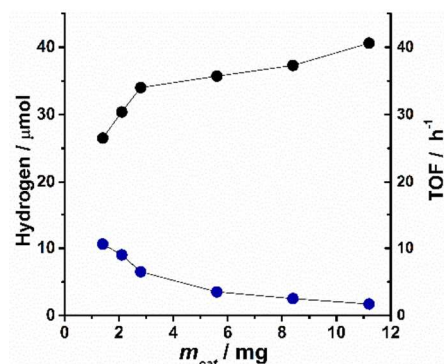


**Fig. 6** Time dependence of TOF (blue dot) and the amount of hydrogen (black dot) photogenerated in the presence of FI (2 mM) and TEA (15%) in water when the amount of  $[\text{Ni}_2(\text{PymS})_4]_n$  changes from 1.4 to 11.2 mg.

In order to investigate the photo-induced electron transfer (PET) process, cyclic voltammetry experiments were carried out in 0.1M sodium perchlorate solution. The  $[\text{Ni}_2(\text{PymS})_4]_n$  was drop-casted on surface of the working electrode and dried by using infrared lamp before the test. As shown in Fig. 7, the first reduction peak appeared at  $-0.83 \text{ V}$ , which was assigned to the single electron transfer from  $\text{Ni}^{\text{II}}\text{Ni}^{\text{II}}$  to  $\text{Ni}^{\text{I}}\text{Ni}^{\text{II}}$ .<sup>27</sup> It has been known that the oxidative potentials of  ${}^1\text{FI}^*$  and  $\text{FI}^-$  are  $-1.7$  and  $-1.3 \text{ V}$ , respectively.<sup>12b,27</sup> If the oxidative quenching happens, the Gibbs free energy of the PET process ( $\Delta G_{\text{ox}} = -0.87 \text{ eV}$ ) is less than zero, which means that the transfer of electrons from  ${}^1\text{FI}^*$  to the catalyst is thermodynamically feasible. Meanwhile, the Gibbs free energy of the reductive PET process ( $\Delta G_{\text{re}} = -0.47 \text{ eV}$ ) is also negative, suggesting that the reductive PET path is also thermodynamically viable. Thus, the excited specie  ${}^1\text{FI}^*$  may be firstly quenched by TEA to form  $\text{FI}^-$ , which then transfer electrons into the catalyst to return to its ground state. Consequently, both of the above two paths are doable in the PET process. By contrast, the driving force of the former is much greater than that of the latter. Therefore, we speculate that the oxidative quenching is possibly dominant in the PET process in thermodynamics.

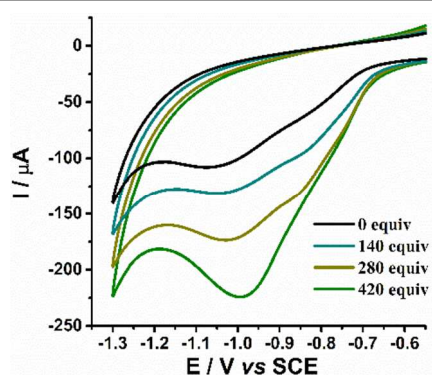


**Fig. 7** CV of  $[\text{Ni}_2(\text{PymS})_4]_n$  (0.1 mg) in the presence of perchloric acid (0–420 equiv.) at a scan rate of  $200 \text{ mVs}^{-1}$ .

To verify the above speculation in PET process, fluorescence quenching experiments were executed in sodium hydroxide aqueous solution at  $\text{pH} = 10$ . When  $[\text{Ni}_2(\text{PymS})_4]_n$  was used in the quenching experiment, the fluorescence intensity of FI gradually decreased with the accumulation of  $[\text{Ni}_2(\text{PymS})_4]_n$  and followed the Stern-Völmer behaviour, which indicates that  $[\text{Ni}_2(\text{PymS})_4]_n$  was an effective quencher by accepting electrons from  $^1\text{FI}^*$ . The oxidative quenching constant  $K_{\text{sv,o}}$  is  $3989.71 \text{ M}^{-1}$ , calculated from the linear region of  $I_0/I$  vs  $[[\text{Ni}_2(\text{PymS})_4]_n]$  (Fig. 8). When TEA was used to replace  $[\text{Ni}_2(\text{PymS})_4]_n$  in the quenching experiment, another Stern-Völmer plot was obtained and the reductive quenching constant  $K_{\text{sv,r}}$  was calculated to be  $15.15 \text{ M}^{-1}$  (Fig. S7), which suggested that  $^1\text{FI}^*$  could also be effectively quenched by TEA through adopting electrons from TEA to form  $\text{FI}^-$ . Therefore, either oxidative or reductive PET path is apparently reasonable. In comparison,  $K_{\text{sv,o}}$  is two orders of magnitude larger than  $K_{\text{sv,r}}$ , which implies that  $[\text{Ni}_2(\text{PymS})_4]_n$  is a much more competitive quencher than TEA. Based on the comprehensive consideration of both CV data and fluorescence spectrometry, we can conclude that the chance of oxidative path is much higher than that of reductive path, and the electron obtained by the catalyst is most likely to come from  $^1\text{FI}^*$ , rather than  $\text{FI}^-$ .

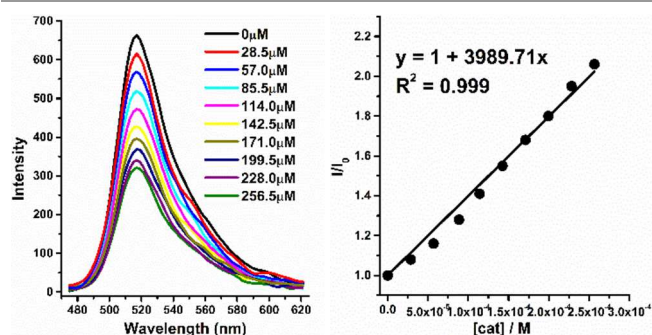
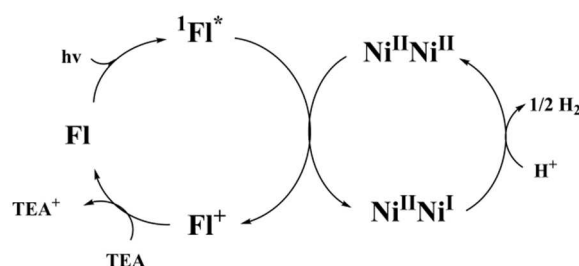


**Fig. 8** Emission quenching (left) and Stern-Volmer plot (right) of FI (0.01 mM) by  $[\text{Ni}_2(\text{PymS})_4]_n$  in water at  $\text{pH} = 10$ .

In CV, a second irreversible reductive peak was observed at around  $-1.07 \text{ V}$ , which might be attributed to the second electron transfer from  $\text{Ni}^{\text{I}}\text{Ni}^{\text{II}}$  to  $\text{Ni}^{\text{I}}\text{Ni}^{\text{I}}$ .<sup>24b, 27</sup> As perchloric acid

was successively added to the system, the current of both two reduction peaks grew dramatically (Fig. 7), which indicated that the catalyst could effectively catalyse hydrogen production in the presence of protons.



**Scheme 1** Proposed pathway for the photocatalytic  $\text{H}_2$  evolution by  $[\text{Ni}_2(\text{PymS})_4]_n$  under white LED irradiation.

According to the above analysis, the total catalytic process was proposed and illustrated in Scheme 1. Under visible illumination, electron transfer from the ground state of FI to the excited state occurred to form  $^1\text{FI}^*$ , which was then oxidatively quenched by  $[\text{Ni}_2(\text{PymS})_4]_n$  to form  $\text{FI}^+$ . Next,  $\text{FI}^+$  was reduced by TEA to regenerate FI and complete the photochemical cycle. Meanwhile, the catalyst obtained electrons from  $^1\text{FI}^*$  to form  $[\text{Ni}_2(\text{PymS})_4]_n^-$ , which catalysed protons in solution to release hydrogen and reproduce  $[\text{Ni}_2(\text{PymS})_4]_n$ . The catalytic circle was fulfilled.

## Conclusions

In this work, we have explored a new non-precious-metal heterogeneous system for photocatalytic hydrogen generation by using a 2D Ni/S metal-organic framework whose dimeric nickel building unit is similar to the active centre of the  $[\text{NiFe}]$ -hydrogenases. This MOF shows a high stability in water over a wide range of pH and efficient catalytic activity in aqueous solution for the photocatalytic hydrogen production under illumination of LED or direct sunlight. The turnover frequency of  $[\text{Ni}_2(\text{PymS})_4]_n$  can reach up to  $10.6 \text{ h}^{-1}$  and the catalyst can be reused in the presence of fresh fluorescein and triethylamine under illumination. In this system, the amount of hydrogen produced was greatly influenced by the pH value, electron donor, dye, and the particle size and amount of the catalyst. An oxidative quenching process was verified in the PET process from CV and fluorescence spectra. In addition, the total cyclic mechanism was proposed by both photochemical and electrochemical analysis. Our approach by using bio-inspired/biomimetic MOFs as heterogeneous photocatalysts pave the way for exploring new materials for direct solar to hydrogen conversion.

## Acknowledgements

We thank the National Basic Research Program of China (973 Program, 2012CB821702), the National Natural Science Foundation of China (21233009 and 21173221) and the State Key Laboratory of Structural Chemistry, Fujian Institute of

Research on the Structure of Matter, Chinese Academy of Sciences for financial support.

## Notes and references

<sup>a</sup> State Key Laboratory of Structural Chemistry, Fujian Institute of Research on the Structure of Matter, Chinese Academy of Sciences, Fujian, Fuzhou 350002, P. R. China. Fax: (+86) 591 83709470; E-mail: [svdu@fjirsm.ac.cn](mailto:svdu@fjirsm.ac.cn)

<sup>b</sup> State Key Laboratory of Physical Chemistry of Solid Surfaces, College of Chemistry and Chemical Engineering, Xiamen University, Xiamen 361005, China.

<sup>c</sup> University of Chinese Academy of Sciences, Beijing 100039, P. R. China.

<sup>d</sup> Key Laboratory of Optoelectronic Materials Chemistry and Physics, Fujian Institute of Research on the Structure of Matter, Chinese Academy of Sciences, Fuzhou, Fujian 350002, China

† Electronic Supplementary Information (ESI) available: IR, PXRD and fluorescence spectra, diagrams for the volume of hydrogen generation vs. pH, particle size and the amount of FI and TEA. Table of TOF for the catalyst. For ESI in electronic format see DOI: 10.1039/b000000x/

- 1 (a) X. Chen, S. Shen, L. Guo and S. S. Mao, *Chem. Rev.*, 2010, **110**, 6503; (b) A. Fujishima and K. Honda, *Nature*, 1972, **238**, 37.
- 2 (a) B. Ginovska-Pangovska, A. Dutta, M. L. Reback, J. C. Linehan and W. J. Shaw, *Acc. Chem. Res.*, 2014, **47**, 2621; (b) A. Kudo and Y. Miseki, *Chem. Soc. Rev.*, 2009, **38**, 253.
- 3 (a) J. P. McEvoy and G. W. Brudvig, *Chem. Rev.*, 2006, **106**, 4455; (b) M. G. Walter, E. L. Warren, S. W. B. James R. McKone, Qixi Mi, Elizabeth A. Santori, and a. N. S. Lewis, *Chem. Rev.*, 2010, **110**, 6446; (c) X. Zhang, Y. Liu and Z. Kang, *ACS Appl. Mater. Interfaces*, 2014, **6**, 4480.
- 4 (a) X. B. Li, Z. J. Li, Y. J. Gao, Q. Y. Meng, S. Yu, R. G. Weiss, C. H. Tung and L. Z. Wu, *Angew. Chem., Int. Ed.*, 2014, **53**, 2085; (b) Y. Sun, J. Sun, J. R. Long, P. Yang and C. J. Chang, *Chem. Sci.*, 2013, **4**, 118.
- 5 (a) T. Nann, S. K. Ibrahim, P. M. Woi, S. Xu, J. Ziegler and C. J. Pickett, *Angew. Chem., Int. Ed.*, 2010, **49**, 1574; (b) C.-B. Li, Z.-J. Li, S. Yu, G.-X. Wang, F. Wang, Q.-Y. Meng, B. Chen, K. Feng, C.-H. Tung and L.-Z. Wu, *Energy Environ. Sci.*, 2013, **6**, 2597.
- 6 (a) Z. Han, L. Shen, W. W. Brennessel, P. L. Holland and R. Eisenberg, *J. Am. Chem. Soc.*, 2013, **135**, 14659; (b) T. Lazarides, T. McCormick, P. Du, G. Luo, B. Lindley and R. Eisenberg, *J. Am. Chem. Soc.*, 2009, **131**, 9192; (c) T. M. McCormick, B. D. Calitree, A. Orchard, N. D. Kraut, F. V. Bright, M. R. Detty and R. Eisenberg, *J. Am. Chem. Soc.*, 2010, **132**, 15480.
- 7 (a) T. Yu, Y. Zeng, J. Chen, Y. Y. Li, G. Yang and Y. Li, *Angew. Chem., Int. Ed.*, 2013, **52**, 5631; (b) W. R. McNamara, Z. Han, P. J. Alperin, W. W. Brennessel, P. L. Holland and R. Eisenberg, *J. Am. Chem. Soc.*, 2011, **133**, 15368.
- 8 (a) H. Y. Wang, W. G. Wang, G. Si, F. Wang, C. H. Tung and L. Z. Wu, *Langmuir*, 2010, **26**, 9766; (b) W. R. McNamara, Z. Han, C.-J. M. Yin, W. W. Brennessel, P. L. Holland and R. Eisenberg, *PNAS*, 2012, **109**, 15594.
- 9 (a) Z. Han and R. Eisenberg, *Acc. Chem. Res.*, 2014, **47**, 2537; (b) M. Wang and L. Sun, *ChemSusChem*, 2010, **3**, 551; (c) P. Du and R. Eisenberg, *Energy Environ. Sci.*, 2012, **5**, 6012.
- 10 (a) P. A. Summers, J. Dawson, F. Ghiotto, M. W. D. Hanson-Heine, K. Q. Vuong, E. S. Davies, X. Z. Sun, N. A. Besley, J. McMaster, M. W. George and M. Schröder, *Inorg. Chem.*, 2014, **53**, 4430; (b) C. He, J. Wang, L. Zhao, T. Liu, J. Zhang and C. Duan, *Chem. Commun.*, 2013, **49**, 627; (c) X. Li, M. Wang, L. Chen, X. Wang, J. Dong and L. Sun, *ChemSusChem*, 2012, **5**, 913.
- 11 (a) C. Orain, F. Quentel and F. Gloaguen, *ChemSusChem*, 2014, **7**, 638-643; (b) X. Li, M. Wang, D. Zheng, K. Han, J. Dong and L. Sun, *Energy Environ. Sci.*, 2012, **5**, 8220.
- 12 (a) J. X. Jian, Q. Liu, Z. J. Li, F. Wang, X. B. Li, C. B. Li, B. Liu, Q. Y. Meng, B. Chen, K. Feng, C. H. Tung and L. Z. Wu, *Nat. Commun.*, 2013, **4**, 2695; (b) Z. Han, W. R. McNamara, M. S. Eum, P. L. Holland and R. Eisenberg, *Angew. Chem., Int. Ed.*, 2012, **51**, 1667.
- 13 (a) H. Zhang, P. Lin, X. Shan, F. Du, Q. Li and S. Du, *Chem. Commun.*, 2013, **49**, 2231; (b) H. Zhang, X. Shan, Z. Ma, L. Zhou, M. Zhang, P. Lin, S. Hu, E. Ma, R. Li and S. Du, *J. Mater. Chem. C.*, 2014, **2**, 1367; (c) Z. Wei, Z. Gu, R. K. Arvapally, Y. P. Chen, R. N. McDougald, Jr., J. F. Ivy, A. A. Yakovenko, D. Feng, M. A. Omary and H. C. Zhou, *J. Am. Chem. Soc.*, 2014, **136**, 8269.
- 14 (a) C. B. Tian, R. P. Chen, C. He, W. J. Li, Q. Wei, X. D. Zhang and S. W. Du, *Chem. Commun.*, 2014, **50**, 1915; (b) Q. Li, C. Tian, H. Zhang, J. Qian and S. Du, *CrystEngComm*, 2014, **16**, 9208.
- 15 (a) M. Du, C. P. Li, M. Chen, Z. W. Ge, X. Wang, L. Wang and C. S. Liu, *J. Am. Chem. Soc.*, 2014, **136**, 10906; (b) T. Zhang and W. Lin, *Chem. Soc. Rev.*, 2014, **43**, 5982.
- 16 (a) L. Li, S. Zhang, L. Xu, J. Wang, L.-X. Shi, Z.-N. Chen, M. Hong and J. Luo, *Chem. Sci.*, 2014, **5**, 3808; (b) S. Wang, W. Yao, J. Lin, Z. Ding and X. Wang, *Angew. Chem., Int. Ed.*, 2014, **53**, 1034; (c) Y. Fu, D. Sun, Y. Chen, R. Huang, Z. Ding, X. Fu and Z. Li, *Angew. Chem., Int. Ed.*, 2012, **51**, 3364.
- 17 (a) L. Li, H. Zhao, J. Wang and R. Wang, *ACS Nano*, 2014, **8**, 5352; (b) C. Wang, K. E. deKrafft and W. Lin, *J. Am. Chem. Soc.*, 2012, **134**, 7211.
- 18 (a) C. G. Silva, I. Luz, F. X. Llabrés i Xamena, A. Corma and H. García, *Chem.–Eur. J.*, 2010, **16**, 11133; (b) T. Zhou, Y. Du, A. Borgna, J. Hong, Y. Wang, J. Han, W. Zhang and R. Xu, *Energy Environ. Sci.*, 2013, **6**, 3229.
- 19 (a) S. Pullen, H. Fei, A. Orthaber, S. M. Cohen and S. Ott, *J. Am. Chem. Soc.*, 2013, **135**, 16997; (b) H. Fei, S. Pullen, A. d. Wagner, S. Ott and S. M. Cohen, *Chem. Commun.*, 2015, **51**, 66.
- 20 (a) J. M. Falkowski, T. Sawano, T. Zhang, G. Tsun, Y. Chen, J. V. Lockard and W. Lin, *J. Am. Chem. Soc.*, 2014, **136**, 5213; (b) K. Manna, T. Zhang, M. Carboni, C. W. Abney and W. Lin, *J. Am. Chem. Soc.*, 2014, **136**, 13182-13185.
- 21 (a) K. Manna, T. Zhang and W. Lin, *J. Am. Chem. Soc.*, 2014, **136**, 6566; (b) C. Wang, D. Liu and W. Lin, *J. Am. Chem. Soc.*, 2013, **135**, 13222.
- 22 Y. Zhao, M. Hong, Y. Liang, R. Cao, W. Li, J. Weng, and S. Lu, *Chem. Commun.*, 2001, **37**, 1020.
- 23 M. v. Gastel, J. L. Shaw, A. J. Blake, M. Flores, M. Schröder, J. McMaster and W. Lubitz, *Inorg. Chem.*, 2008, **47**, 11688.
- 24 (a) N. T. Nguyen, Y. Mori, T. Matsumoto, T. Yatabe, R. Kabe, H. Nakai, K.-S. Yoon and S. Ogo, *Chem. Commun.*, 2014, **50**, 13385; (b) L. C. Song, J. P. Li, Z. J. Xie and H. B. Song, *Inorg. Chem.*, 2013, **52**, 11618; (c) L. C. Song, Y. L. Li, L. Li, Z. C. Gu and Q. M. Hu, *Inorg. Chem.*, 2010, **49**, 10174.
- 25 (a) X. L. Hu, C. Y. Sun, C. Qin, X. L. Wang, H. N. Wang, E. L. Zhou, W. E. Li and Z. M. Su, *Chem. Commun.*, 2013, **49**, 3564; (b) P. Huang, C. Qin, Z. M. Su, Y. Xing, X. L. Wang, K. Z. Shao, Y. Q. Lan and E. B. Wang, *J. Am. Chem. Soc.*, 2012, **134**, 14004; (c) A. Fateeva, P. A.



- Chater, C. P. Ireland, A. A. Tahir, Y. Z. Khimyak, P. V. Wiper, J. R. Darwent and M. J. Rosseinsky, *Angew. Chem., Int. Ed.*, 2012, **51**, 7440.
- 26 D. Ding, K. Li, B. Liu and B. Z. Tang, *Acc. Chem. Res.*, 2014, **46**, 2441.
- 27 H. H. Cui, J. Y. Wang, M. Q. Hu, C. B. Ma, H. M. Wen, X. W. Song and C. N. Chen, *Dalton Trans.*, 2013, **42**, 8684.